Chapter 1—
Introduction

1.1—
Introduction

The twin subjects of fractal geometry and chaotic dynamics have been behind an enormous change in the way scientists and engineers perceive, and subsequently model, the world in which we live. Chemists, biologists, physicists, physiologists, geologists, economists, and engineers (mechanical, electrical, chemical, civil, aeronautical etc) have all used methods developed in both fractal geometry and chaotic dynamics to explain a multitude of diverse physical phenomena: from trees to turbulence, cities to cracks, music to moon craters, measles epidemics, and much more. Many of the ideas within fractal geometry and chaotic dynamics have been in existence for a long time, however, it took the arrival of the computer, with its capacity to accurately and quickly carry out large repetitive calculations, to provide the tool necessary for the in-depth exploration of these subject areas. In recent years, the explosion of interest in fractals and chaos has essentially ridden on the back of advances in computer development.

The objective of this book is to provide an elementary introduction to both fractal geometry and chaotic dynamics. The book is split into approximately two halves: the first—chapters 2–4—deals with fractal geometry and its applications, while the second—chapters 5–7—deals with chaotic dynamics. Many of the methods developed in the first half of the book, where we cover fractal geometry, will be used in the characterization (and comprehension) of the chaotic dynamical systems encountered in the second half of the book. In the rest of this chapter brief introductions to fractal geometry and chaotic dynamics are given, providing an insight to the topics covered in subsequent chapters of the book.

1.2—
A Matter of Fractals

In recent years, the science of fractal geometry has grown into a vast area of knowledge, with almost all branches of science and engineering gaining from the new insights it has provided. Fractal geometry is concerned with the properties of fractal objects, usually simply known as **fractals.** Fractals may be found in nature or generated using a mathematical recipe. The word 'fractal' was coined by Benoit Mandelbrot, sometimes referred to as the father of fractal geometry. Mandelbrot realized that it is very often

impossible to describe nature using only Euclidean geometry, that is in terms of straight lines, circles, cubes, and such like. He proposed that fractals and fractal geometry could be used to describe real objects, such as trees, lightning, river meanders and coastlines, to name but a few.

There are many definitions of a fractal. Possibly the simplest way to define a fractal is as an object *which appears self-similar under varying degrees of magnification. In effect, possessing symmetry across scale, with each small part of the object replicating the structure of the whole.* This is perhaps the loosest of definitions, however, it captures the essential, defining characteristic, that of **self-similarity.** A diagram is possibly the best way to illustrate what is meant by a fractal object. Figure 1.1 contains sketches of two naturally occurring 'objects': an island coastline and a person. As we zoom into the coastline, we find that its ruggedness is repeated on finer and finer scales, and under rescaling looks essentially the same: the coastline is a fractal curve. The person, however, is not a self-similar object. As we zoom into various parts of the body, we see quite different forms. The hand does not resemble the whole body, the fingernail does not look like the hand and so on. Even viewing different parts of the body at the same scale, say the hand and the head, we would see that again they are not similar in form. We conclude that a person is not a fractal object. It is interesting to note at this stage that, although the body as a whole is not a fractal object, recent studies have attempted, with some success, to characterize certain parts of the body using fractal geometry, for example, the branching structure of the lung and the fine structure of the neuron (brain cell).

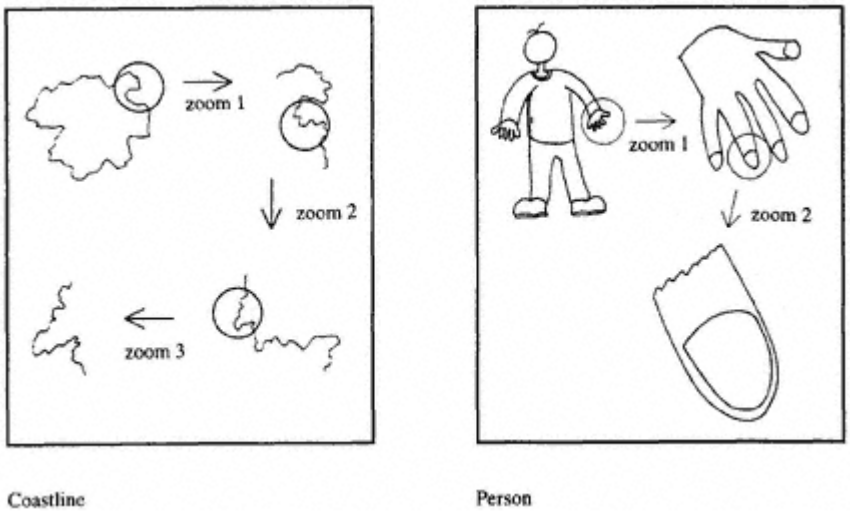

Figure 1.1.
Fractal and non-fractal objects.

Figure 1.2 contains four **natural fractals:** the boundary of clouds, wall cracks, a hillside silhouette and a fern. All four possess self-similarity. The first three natural fractals possess the same statistical properties (i.e. the same degree of ruggedness) as we zoom in. They possess **statistical self-similarity.** On the other hand, the fern possesses

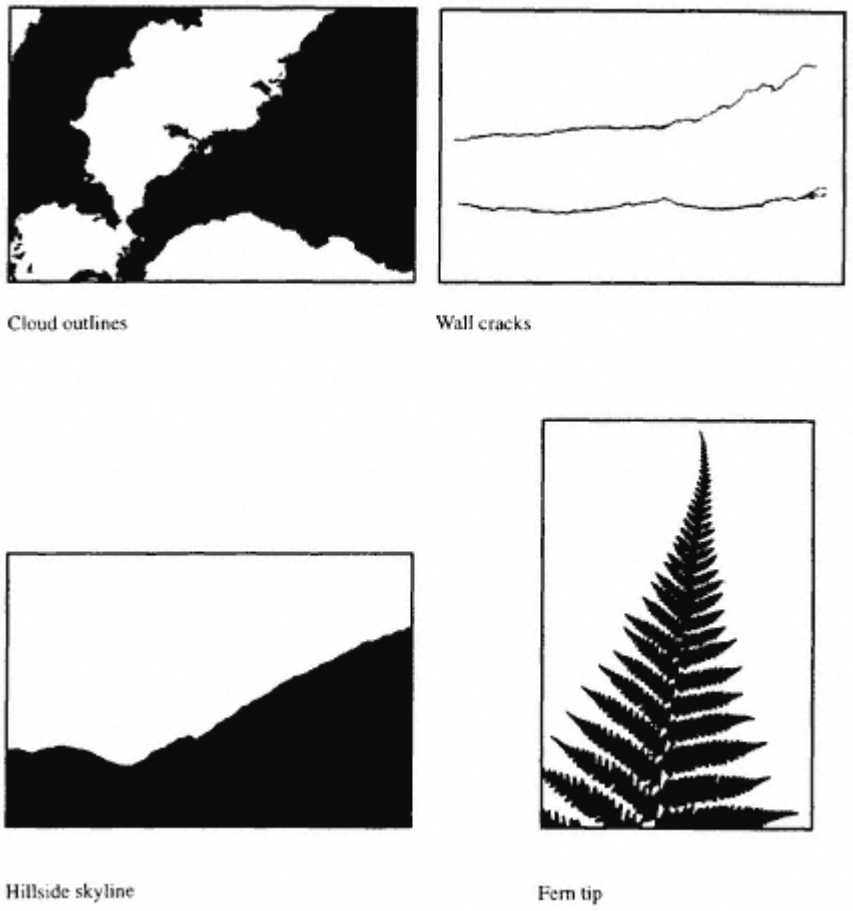

Figure 1.2.
Natural fractal objects.

exact self-similarity. Each frond of the fern is a mini-copy of the whole fern, and each frond branch is similar to the whole frond, and so on. In addition, as we move towards the top of the fern we see a smaller and smaller copy of the whole fern. The fractals of figure 1.2 require a two-dimensional (2D) plane to 'live in', that is all the points on them can be specified using only two co-ordinates. Put more formally, they have a Euclidean dimension of two. However, many natural fractals need a 3D world in which to exist. Take, for example, a tree whose branches weave through three dimensions; see the tree branching in 3D in figure 1.3 (if you can!). Fractals themselves have their own dimension, known as the **fractal dimension,** which is usually (but not always) a noninteger dimension that is greater than their topological dimension, D_T, and less than their Euclidean dimension D_E (see chapter 2). There are many definitions of fractal dimension and we shall encounter a number of them as we proceed through the text, including: the similarity dimension, D_S; the divider dimension, D_D; the Hausdorff dimension, D_H; the box counting dimension, D_B; the correlation dimension, D_C; the information

dimension, D_I; the pointwise dimension D_P; the averaged pointwise dimension, D_A; and the Lyapunov dimension D_L. The last seven dimensions listed are particularly useful in characterizing the fractal structure of strange attractors associated with chaotic dynamics.

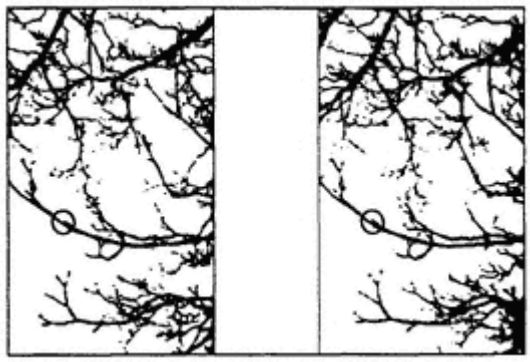

Figure 1.3.
Tree branching in 3D. To see the 3D image, illuminate the page with a good even source of light: daylight is by far the best. Keeping the page still, view the images from a distance of 15–20 cm, let your eyes relax and try to merge the two circles. After merging, the image should come into focus within a few seconds. Once focused, let your eyes wander around the image to see 3D. The technique needs a little practice: the trick is to focus on the merged image without the two constituent images diverging, but persistence usually pays off.

We make one more important distinction between fractals which are self-similar everywhere and those which are self-similar only if we look in the right place. Examples are given in figure 1.4. The figure contains three **mathematical fractals,** these are: a logarithmic spiral, a binary tree, and a Sierpinski gasket. We see self-similarity in the logarithmic spiral of figure 1.4(*a*) only if we zoom into its point of convergence. The part of the spiral contained within box A contains the point of convergence, hence infinitely many scaled copies of the spiral exist within this area. However, the part of the spiral within box B does not contain the point of convergence and hence does not contain scaled down replicas of the whole log spiral. The binary tree (figure 1.4(*b*)) is simple to construct mathematically: we simply add further, scaled down, T-shaped branches to the ends of the previous branches. After an infinite number of branch additions we have the binary tree. As we zoom into the branches of the binary tree we see more and more detail, consisting of exactly self-similar copies of the whole tree. Hence, it is a fractal. However, the self-similarity of the binary tree (figure 1.4(*b*)) is only evident if we zoom into one of its branch ends. The circled area A contains one such branch end, which is an exact copy of the whole tree scaled down by one eighth. Contrast this with the part of the tree contained within the circled area B which is not a scaled down copy of the whole tree. The Sierpinski gasket of figure 1.4(*c*) (the construction of which is detailed in chapter 2) is self-similar everywhere. No matter where we zoom into the gasket, we will see further copies of the whole gasket. This property is known as **strict self-similarity** and the Sierpinski gasket is a strictly self-similar fractal. In this book we will concentrate on strictly self-similar fractals. In figure 1.2 the cloud boundary, wall

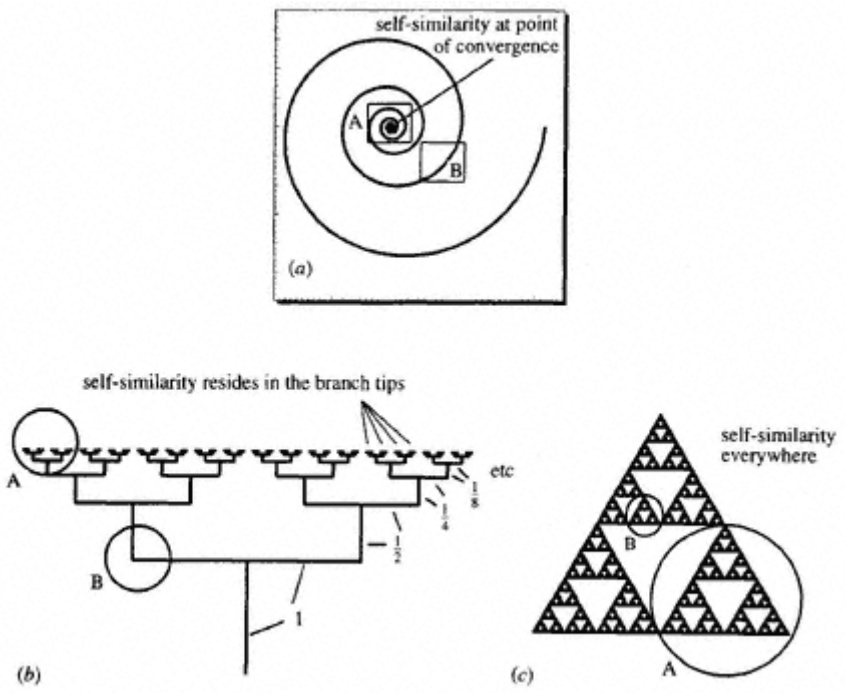

Figure 1.4.
The nature of self-similarity. (*a*) The log spiral is self-similar only at its point of convergence. (*b*) The binary tree is self-similar only at the branch tips. (*c*) The Sierpinski gasket is self-similar everywhere.

crack, and hillside skyline are strictly self-similar, whereas the fern of figure 1.2 and the tree of figure 1.3 are only self-similar at their branch ends.

One last point worth noting is that even the best examples of natural fractals do not possess self-similarity at all scales, but rather over a sufficiently large range to allow fractal geometric methods to be successfully employed in their description. On the other hand, mathematical fractals can be specified to infinite precision and are thus self-similar at all scales. The distinction between the two is usually blurred in the literature, however, it is one worth remembering if you intend using, in a practical situation, some of the methods from fractal geometry learned from this text.

1.3— Deterministic Chaos.

Oscillations are to be found everywhere in science and nature. The mechanical engineer may be concerned with the regular oscillation of an out of balance drive shaft; the civil engineer with the potentially disastrous structural vibrations induced by vortex shedding on a bridge deck; the electrical engineer with the oscillatory output from nonlinear circuits; the chemist/chemical engineer with the regular cycling of a chemical reaction; the geologist/geophysicist with earthquake tremors; the biologist with the cycles of growth and decay in animal populations; the cardiovascular surgeon with the regular

(and more so, irregular) beating of the human heart; the economist with the boom—bust cycles of the stock market; the physicist with the oscillatory motion of a driven pendulum; the astronomer with the cyclical motion of celestial bodies; and so on. (The list is extensive and diverse!)

Dynamical oscillators may be classified into two main categories: linear and nonlinear. In general, all real systems are nonlinear, however, very often it is the case that, as a first approximation to the dynamics of a particular system, a linear model may be used. Linear models are preferable from a scientist's point of view as typically they are much more amenable to mathematical analysis. (Hence the disproportionate number of linear systems studied in science.) Nonlinear systems, in contrast, are much more difficult to analyse mathematically, and, apart from a few exceptions, analytical solutions are not possible for the nonlinear differential equations used to describe their temporal evolution. In addition, only nonlinear systems are capable of a most fascinating behaviour known as **chaotic motion,** or simply **chaos,** whereby even simple nonlinear systems can, under certain operating conditions, behave in a seemingly unpredictable manner.

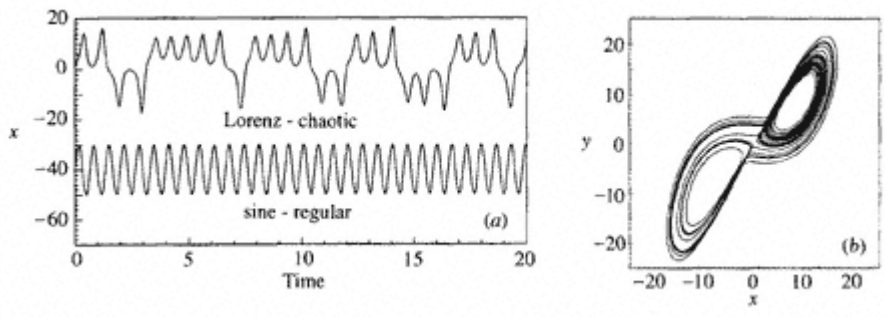

Figure 1.5.
Chaos and regularity. (*a*) Time series of the chaotic Lorenz model and a periodic sinusoidal waveform. (*b*) Phase portrait of the Lorenz strange attractor.

In 1963 Edward Lorenz published his work entitled 'Deterministic nonperiodic flow' which detailed the behaviour of a simplified mathematical model representing the workings of the atmosphere. Lorenz showed how a relatively simple, **deterministic** mathematical model (that is, one with no randomness associated with it) could produce apparently unpredictable behaviour, later named chaos. The Lorenz model (see chapter 6) contains three variables: x, y and z. Figure 1.5(a) shows a chaotic time series output of the x variable of the Lorenz model. Notice that there is a recognizable structure to the time series: first the system oscillates in the positive-x region for a couple of oscillations, then it switches over to the negative x-region for a couple of oscillations, then back to the positive x-region for a few oscillations, and so on. However, the system never exactly repeats its behaviour. It would not matter how long we let the Lorenz model run for, we would never come across a repetition in the waveform. It is this aperiodic behaviour that is known as chaos. Compare it to the regular, periodic oscillations of the sinusoidal waveform (plotted below the Lorenz output) which repeats itself exactly and indefinitely. By plotting the Lorenz variables against each other, rather than against time, we can produce compact pictures of the system's dynamics. In two dimensions these are

known as phase portraits. The phase portrait for the Lorenz time series is shown in figure 1.5(*b*). Starting the Lorenz system from many initial conditions produces phase portraits all of the same form: the system is attracted towards this type of final solution. Figure 1.5(*b*) is then a plot of the long term behaviour of the Lorenz system and is known as the attractor of the system. If we zoom into the fine scale structure of the attractor for the chaotic Lorenz system we see that it has a fractal structure. The attractors for chaotic systems which have a fractal structure are termed **strange attractors.** The fractal structure of strange attractors may be examined using one or more of the definitions of fractal dimension mentioned in the above section. (See chapter 7 for more details.)

Chaos has now been found in all manner of dynamical systems; both mathematical models and, perhaps more importantly, natural systems. Chaotic motion has been observed in all of the 'real' oscillatory systems cited at the beginning of this section. In addition, many common qualitative and quantitative features can be discerned in the chaotic motion of these systems. This ubiquitous nature of chaos is often referred to as the **universality** of chaos.

1.4— Chapter Summary and Further Reading

1.4.1— Chapter Keywords and Key Phrases

fractals	*self-similarity*	*natural fractals*
statistical self-similarity	*exact self-similarity*	*fractal dimension*
mathematical fractals	*strict self-similarity*	*chaotic motion/chaos*
deterministic models	*strange attractors*	*universality*

1.4.2— Further Reading

Non-mathematical treatments of the history and role of fractals and chaos in science, engineering and mathematics can be found in the books by Gleick (1987), Stewart (1989), Briggs and Peat (1989), Lorenz (1993) and Ruelle (1993). Also worth consulting is the highly readable collection of non-mathematical papers by leading experts from various fields edited by Hall (1992). The explosion in the number of scientific articles relating to chaos and fractals is shown graphically by Pickover (1992). Simple computer programs to generate a range of fractal and chaotic phenomena are given in the text by Bessant (1993). Other forms of medium worth consulting are the videos by Barlow and Gowan (1988) and Peitgen *et al* (1990), and also the freeware software package FRACTINT, widely available on the internet, user friendly, and of excellent quality. In fact, a search on the world wide web using the keywords 'fractal' or 'chaos' should yield a large amount of material, much of which is at a reasonably elementary level.

Chapter 2—
Regular Fractals and Self-Similarity

2.1—
Introduction

In this chapter we will examine some common mathematical fractals with structures comprising of exact copies of themselves at all magnifications. These objects possess **exact self-similarity** and are known as **regular fractals.** In chapter 1, a fractal object was loosely defined as one which appears self-similar at various scales of magnification and also as an object with its own **fractal dimension,** which is usually (but not always) a non-integer dimension greater than its topological dimension, D_T, and less than its Euclidean dimension, D_E. To date, there exists no watertight definition of a fractal object. Mandelbrot offered the following definition: 'A fractal is by definition a set for which the Hausdorff dimension strictly exceeds the topological dimension', which he later retracted and replaced with: 'A fractal is a shape made of parts similar to the whole in some way'. In this book, we will adopt, as a *test for a fractal object, the condition that its fractal dimension exceeds its topological dimension—whichever measure of fractal dimension is employed.* As we do this, bear in mind the ambiguous nature of the definition of a fractal.

2.2—
The Cantor Set

The **Cantor set** must certainly rank as one of the most frequently quoted fractal objects in the literature, alongside perhaps, the Koch curve and Mandelbrot set. It is arguably the simplest of fractals and a good place to begin our discussion on fractals and their geometric properties. The Cantor set consists of an infinite set of disappearing line segments in the unit interval. The best aid to the comprehension of the Cantor set fractal is an illustration of its method of construction. This is given in figure 2.1 for the simplest form of Cantor set, namely the triadic Cantor set. The set is generated by removing the middle third of the unit line segment (step $k = 1$ in the figure). From the two remaining line segments, each one third in length, the middle thirds are again removed (step $k = 2$ in the figure). The middle thirds of the remaining four line segments, each one-ninth in length, are then removed ($k = 3$) and so on to infinity. What is left is a collection of infinitely many disappearing line segments lying on the unit interval whose individual and combined lengths approach zero. This set of 'points' is known as a Cantor set, Cantor dust, or Cantor discontinuum.

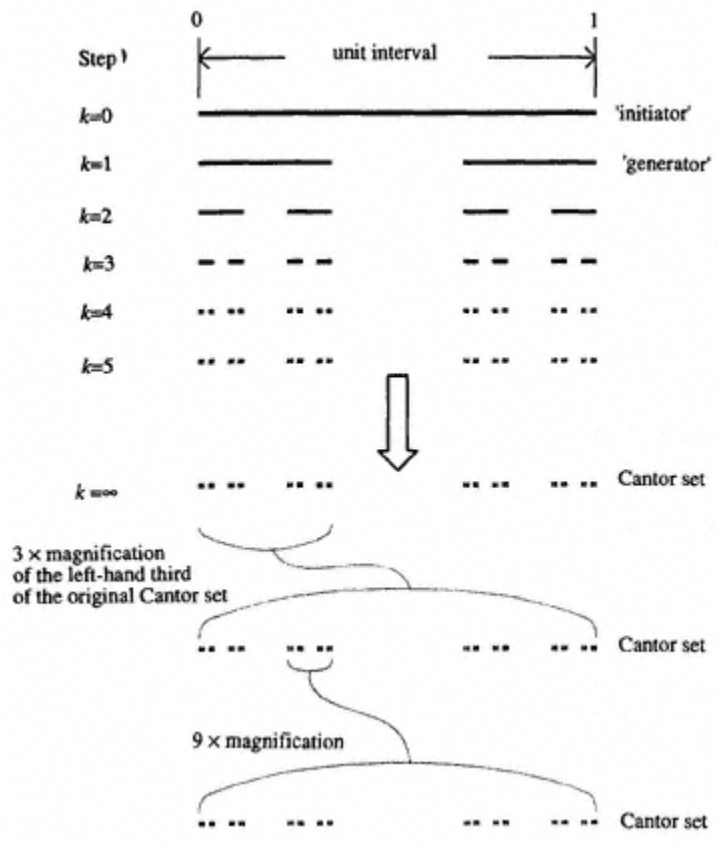

Figure 2.1.
The construction of the triadic Cantor set.

In the construction of the Cantor set the initial unit line segment, $k = 0$, is known as the **initiator** of the set. The first step, $k = 1$, is known as the **generator** (or sometimes motif), as it is the repeated iteration of this step on subsequent line segments which leads to the generation of the set. Notice in the figure that the fifth iteration is indistinguishable from the Cantor set obtained at higher iterations. This problem occurs due to the limit of the finite detail our eyes (or the printer we use to plot the image) can resolve. Thus, to illustrate the set, it is sufficient to repeat the generation process only by the number of steps necessary to fool the eye, and not an infinite number of times. (This is true for all illustrations of fractal objects.) However, make no mistake, only after an infinite number of iterations do we obtain the Cantor set. For a finite number of iterations the object produced is merely a collection of line segments with finite measurable length. These objects formed *en route* to the fractal object are termed **prefractals.**

The Cantor set is a regular fractal object which exhibits exact self-similarity over all scales. This property is illustrated at the bottom of figure 2.1, where the left-hand third of the Cantor set is magnified three times. After magnification we see that the original

Cantor set is formed. Further zooming into one ninth of the newly formed set, we see that again the original set is formed. In fact copies of the Cantor set abound. Zooming into any apparent 'point' in the set produces the original set. It is easily seen that the Cantor set contains an infinite number of copies of itself, within itself, or to put it another way the Cantor set is made up of Cantor sets.

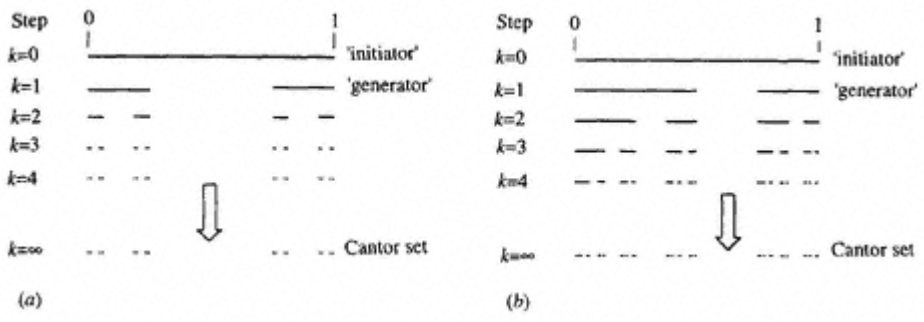

Figure 2.2.
Two more examples of Cantor set construction. (*a*) Middle half removal. (*b*) Two-scale Cantor construction.

The triadic Cantor set described above is so called as it involves the removal of the middle third of the remaining line segments at each step in its construction. Any number of variants of the Cantor set may be formed by changing the form of the generator. Two such Cantor sets are shown in figure 2.2. The set on the left of the figure is formed by removing the middle half of each remaining line segment at each step, leaving the end quarters of the line. In the right-hand construction, the segment of each line removed at each stage leaves the first half of the original line and the last quarter. Again after an infinite number of steps a Cantor set is formed.

The Cantor set is simple in its construction, yet it is an object with infinitely rich structure. How do we make sense of the Cantor set? It does not fill up the unit interval continuously, as a line, i.e. one-dimensional object, nor is it a countable collection of zero-dimensional points. Rather, it fills up the unit interval in a special way and as a complete set has a dimension which is neither zero nor one, in fact it has a non-integer, fractal dimension somewhere in between zero and one. Non-integer, fractal dimensions are quite difficult to conceptualize initially and will be dealt with in the following sections.

2.3—
Non-Fractal Dimensions:
The Euclidean and Topological Dimensions.

Generally, we can conceive of objects that are zero dimensional or 0D (points), 1D (lines), 2D (planes), and 3D (solids) see figure 2.3. We feel comfortable with zero, one, two and three dimensions. We form a 3D picture of our world by combining the 2D images from each of our eyes. Is it possible to comprehend higher-dimensional objects, i.e. 4D, 5D, 6D and so on? What about non-integer-dimensional objects such as 2.12D, 3.79D or 36.91232 . . . D?

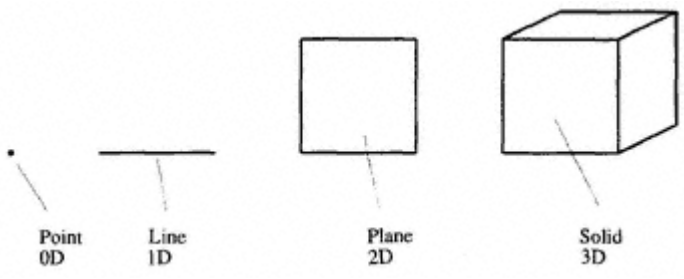

Figure 2.3.
Common integer dimensions.

We will encounter many definitions of dimension as we proceed through this book. Before we deal with fractal dimensions, let us look at the two most common, and perhaps most comprehensible, definitions of dimension, the **Euclidean dimension**, D_E, and **topological dimension,** D_T. Both definitions lead to non-fractal, integer dimensions. The Euclidean dimension is simply the number of co-ordinates required to specify the object. The topological dimension is more involved. The branch of mathematics known as topology considers shape and form of objects from essentially a qualitative point of view. Topology deals with the ways in which objects may be distorted from one shape and formed into another without losing their essential features. Thus straight lines may be transformed into smooth curves or bent into 'crinkly' curves as shown in figure 2.4, where each of the constructions are topologically equivalent. Certain features are invariant under proper transformations (called homeomorphisms by topologists)— for instance, holes in objects remain holes regardless of the amount of stretching and twisting the object undergoes in its transformation from one shape to another. All of the two-holed surfaces in figure 2.5, although quite different in shape, are topologically equivalently as each one may be stretched and moulded into one of the others.

Figure 2.4.
Topologically equivalent curves.

The topological dimension of an object does not change under the transformation of the object. The topological dimension derives from the ability to cover the object with discs of small radius. This is depicted in figure 2.6. The line segment may be covered using many discs intersecting many times with each other (figure 2.6(*a*)). However, it is possible to refine this covering using discs with only a single intersection between adjacent pairs of discs (figure 2.6(*b*)). Even when the line is contorted, one can find

Figure 2.5.
Topologically equivalent forms—surfaces with two holes.

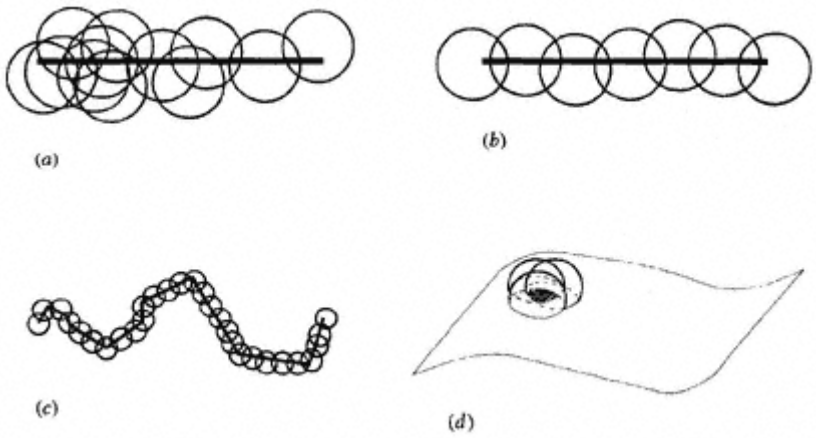

Figure 2.6.
The covering of objects with discs and spheres to reveal the topological dimension. (*a*) Line segment covered by discs. (*b*) Line segment covered by discs only intersecting in pairs. (*c*) Crinkly line covered by discs only intersecting in pairs. (*d*) Surface covered by spheres the intersection region is shaded.

discs sufficiently small to cover it with only intersections occurring between adjacent pairs of the covering discs, depicted in figure 2.6(*c*). The segment within each covering disc can itself be covered using smaller discs which require only to intersect in pairs. In a similar manner, a surface may be covered using spheres of small radius with a minimum number of intersections requiring intersecting triplets of spheres (figure 2.6(*d*)). The definition of the topological dimension stems from this observation. The covering of an object by elements (discs or spheres) of small radius requires intersections between a minimum of $D_T + 1$ groups of elements. Figure 2.7 shows a comprehensive set of common forms with their respective Euclidean and topological dimensions. Figure 2.8 contains the Cantor set. Its Euclidean dimension, D_E, is obviously equal to one, as we require one co-ordinate direction to specify all the points on the set. It can be seen from the figure that it is possible to find single non-intersecting discs of smaller and smaller radius to cover sub-elements of the set, thus the topological dimension, D_T, of the Cantor set is zero.

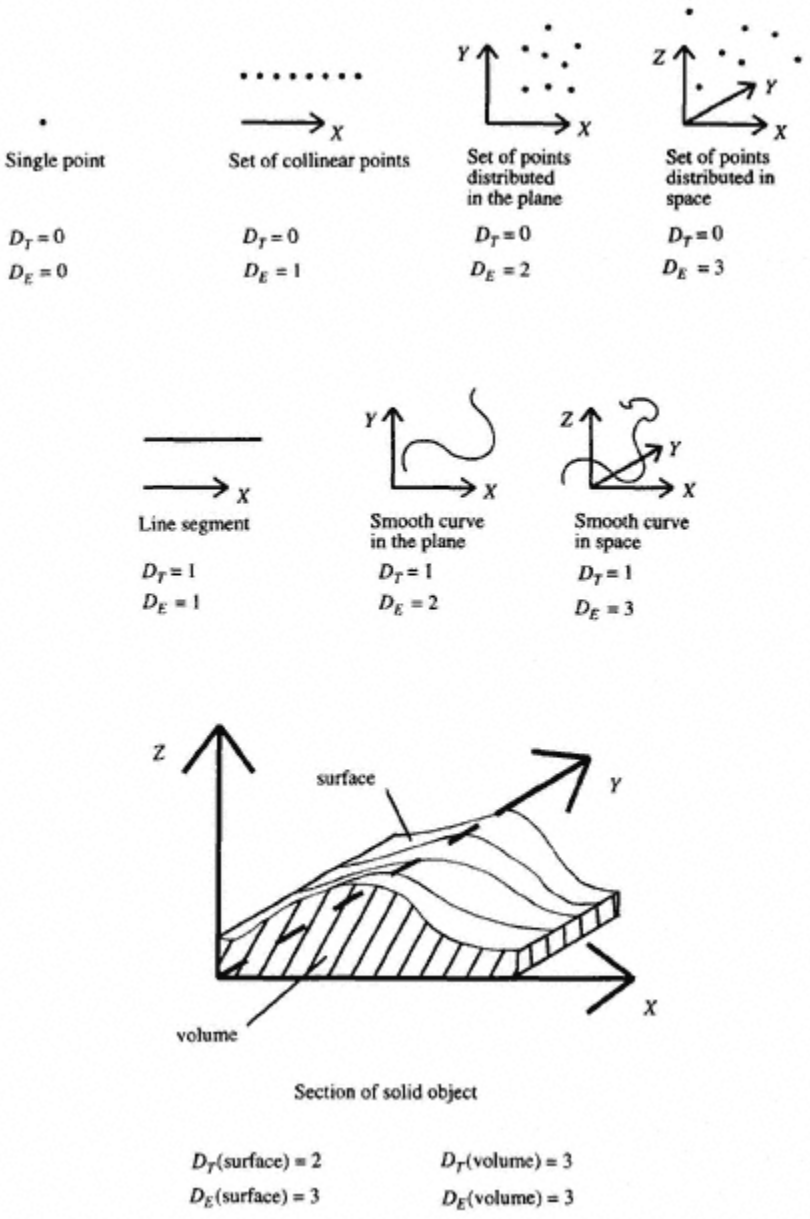

Figure 2.7.
A set of common forms with their respective Euclidean and topological dimensions.

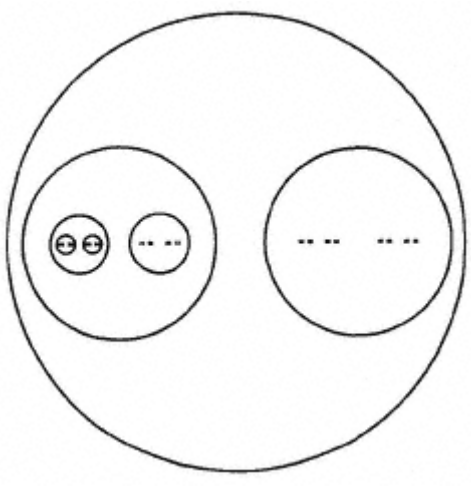

Figure 2.8.
Covering the Cantor set with successively smaller, non-intersecting discs to reveal the topological dimension.

2.4— The Similarity Dimension

Their are many definitions of dimension which give a non-integer, or fractal, dimension. These dimensions are particularly useful in characterizing fractal objects. In the remaining parts of this chapter we will concentrate on the **similarity dimension,** denoted *Ds*, to characterize the construction of regular fractal objects. As we proceed through subsequent chapters of the text further definitions of dimension will be introduced where appropriate.

The concept of dimension is closely associated with that of scaling. Consider the line, surface and solid depicted in figure 2.9, divided up respectively by self-similar sub-lengths, sub-areas and sub-volumes of side length ε. For simplicity in the following derivation assume that the length, L, area, A, and volume, V, are all equal to unity.

Consider first the line. If the line is divided into N smaller self-similar segments, each ε in length, then ε is in fact the scaling ratio, i.e. $\varepsilon/L = \varepsilon$, since $L = 1$. Thus

$$L = N\varepsilon = 1 \qquad (2.1a)$$

i.e. the unit line is composed of N self-similar parts scaled by $\varepsilon = 1/N$.

Now consider the unit area in figure 2.4. If we divide the area again into N segments each ε^2 in area, then

$$A = N\varepsilon^2 = 1 \qquad (2.1b)$$

i.e. the unit surface is composed of N self-similar parts scaled by $\varepsilon = 1/N^{1/2}$.

Applying similar logic, we obtain for a unit volume

$$V = N\varepsilon^3 = 1 \qquad (2.1c)$$

i.e. the unit solid is N self-similar parts scaled by $\varepsilon = 1/N^{1/3}$.

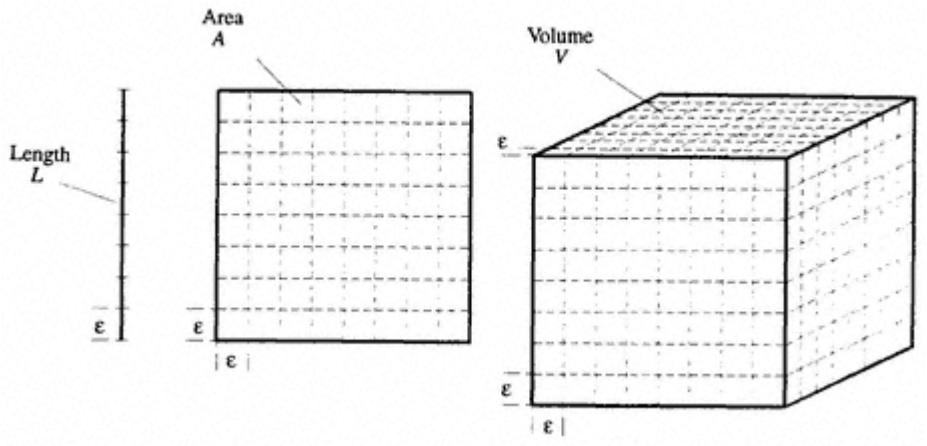

Figure 2.9.
Scaling and dimension. Each object consists of N elements of side length ε, N is determined by the choice of ε. It should be noted that N for each object need not necessarily be the same, as is the case shown above.

Examining expressions (2.1a–c) we see that the exponent of e in each case is a measure of the (similarity) dimension of the object, and we have in general

$$N\varepsilon^{D_S} = 1. \qquad (2.2)$$

Using logarithms leads to the expression,

$$D_S = \frac{\log(N)}{\log(1/\varepsilon)}. \qquad (2.3)$$

Note that here the subscript 'S' denotes the similarity dimension.

The above expression has been derived using familiar objects which have the same integer Euclidean, topological and similarity dimensions, i.e. a straight line, planar surface and solid object, where $D_E = D_S = D_T$. However, equation (2.3) may also be used to produce dimension estimates of fractal objects where D_S is non-integer. This can be seen by applying the above definition of the self-similar dimension to the triadic Cantor set constructed in section 2.2, (see figures 2.1 and 2.8). From figure 2.1 we saw that the left-hand third of the set contains an identical copy of the set. There are two such identical copies of the set contained within the set, thus $N = 2$ and $\varepsilon = \frac{1}{3}$. According to equation (2.3) the similarity dimension is then

$$D_S = \frac{\log(2)}{\log(1/(1/3))} = \frac{\log(2)}{\log(3)} = 0.6309\ldots. \qquad (2.4a)$$

Thus, for the Cantor set, D_S is less than one and greater than zero: in fact it has a non-integer similarity dimension of 0.6309 . . . due to the fractal structure of the object. We saw in the previous section that the Cantor set has Euclidean dimension of one and a topological dimension of zero, thus $D_E > D_S > D_T$. As the similarity dimension

exceeds the topological dimension, according to our test for a fractal given in section 2.1, the set is a fractal with a fractal dimension defined by the similarity dimension of 0.6309. . . . As an aid to comprehension it may be useful to think of the Cantor set as neither a line nor a point, but rather something in between.

Instead of considering each sub-interval of the Cantor set scaled down by one-third we could have looked at each subinterval scaled down by one-ninth. As we saw from figure 2.1, there are four such segments, each an identical copy of the set. In this case $N = 4$ and $\varepsilon = \frac{1}{9}$ and again this leads to a similarity dimension of

$$D_S = \frac{\log(4)}{\log(1/(1/9))} = \frac{\log(4)}{\log(9)} = \frac{2\log(2)}{2\log(3)} = 0.6309\ldots. \qquad (2.4b)$$

Similarly there are eight smaller subintervals containing identical copies of the set each at a scale of 2 of the original set, giving

$$D_S = \frac{\log(8)}{\log(1/(1/27))} = \frac{\log(8)}{\log(27)} = \frac{3\log(2)}{3\log(3)} = 0.6309\ldots \qquad (2.4c)$$

and so on.

By now a general scaling rule is apparent. The general expression for the similarity dimension of the Cantor set is

$$D_S = \frac{\log(2^C)}{\log(3^C)} = \frac{C\log(2)}{C\log(3)} = \frac{\log(2)}{\log(3)} = 0.6309\ldots \qquad (2.4d)$$

where the scaling constant, C, depends on the scale used to identify the self-similarity of the object. It can be seen from the above that the similarity dimension is independent of the scale used to investigate the object.

2.5— The Koch Curve

The **Koch curve,** the method of construction of which is illustrated in figure 2.10, is another well documented fractal. As with the Cantor set, the Koch curve is simply constructed using an iterative procedure beginning with the initiator of the set as the unit line segment (step $k = 0$ in the figure). The unit line segment is divided into thirds, and the middle third removed. The middle third is then replaced with two equal segments, both one-third in length, which form an equilateral triangle (step $k = 1$): this step is the generator of the curve. At the next step ($k = 2$), the middle third is removed from each of the four segments and each is replaced with two equal segments as before. This process is repeated an infinite number of times to produce the Koch curve. Once again the self-similarity of the set is evident: each sub-segment is an exact replica of the original curve, as shown in figure 2.11.

A noticeable property of the Koch curve is that it is seemingly infinite in length. This may be seen from the construction process. At each step, k, in its generation, the length of the prefractal curve increases to $\frac{4}{3}L_{k-1}$, where L_{k-1} is the length of the curve in the preceding step. As the number of generations increase the length of the curve diverges. It is therefore apparent that length is not a useful measure of the Koch curve, as

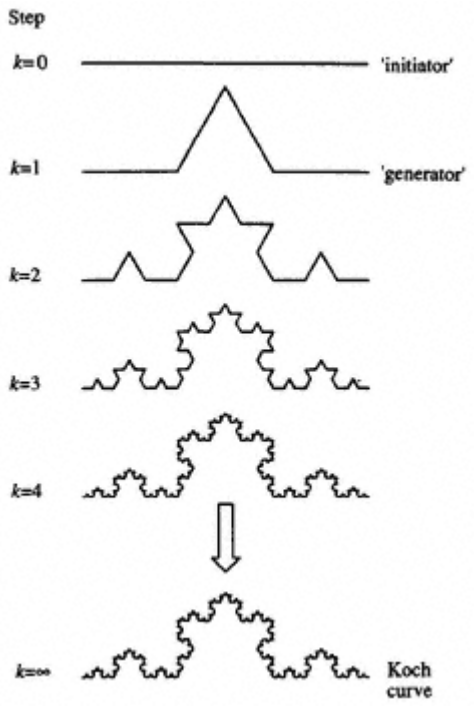

Figure 2.10.
The construction of the Koch curve.

defined in the limit of an infinite number of iterations. In addition, it can be shown that the Koch curve is effectively constructed from corners, hence no unique tangent occurs anywhere upon it. The Koch curve is not a smooth curve and is nowhere-differentiable, as a unique tangent, or slope, cannot be found anywhere upon it.

The Koch curve is a fractal object possessing a fractal dimension. Each smaller segment of the Koch curve is an exact replica of the whole curve. As we can see from figure 2.11, at each scale there are four sub-segments making up the curve, each one a one third reduction of the original curve. Thus, $N = 4$, $\varepsilon = \frac{1}{3}$, and the similarity dimension based on expression (2.3) is

$$D_S = \frac{\log(N)}{\log(1/\varepsilon)} = \frac{\log(4)}{\log(3)} = 1.2618\ldots \qquad (2.5)$$

that is, the Koch curve has a dimension greater than that of the unit line ($D_E = D_T = 1$) and less than that of the unit area ($D_E = D_T = 2$). The Euclidean dimension of the Koch curve, D_E, is two as we need two co-ordinate directions to specify all points on it. The topological dimension, D_T, of the Koch curve is unity , as we can cover it with successively smaller discs intersecting in pairs. The similarity dimension of the Koch curve lies between its Euclidean and topological dimension, i.e. $D_E > D_S > D_T$, which leads us to conclude that it is indeed a fractal object, with a fractal (similarity) dimension, D_S, of 1.2618 . . . .

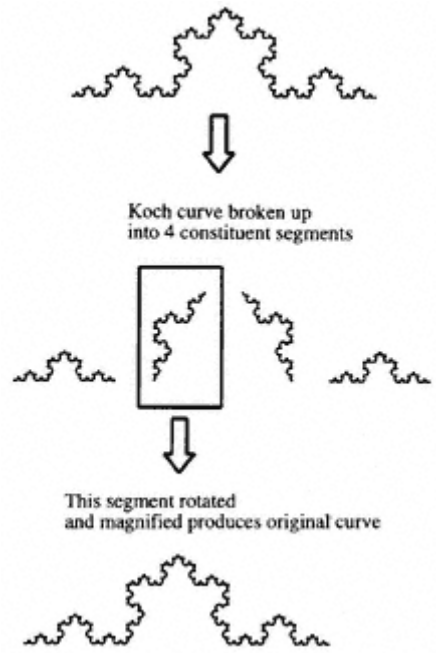

Figure 2.11.
The self-similar structure of the Koch curve.

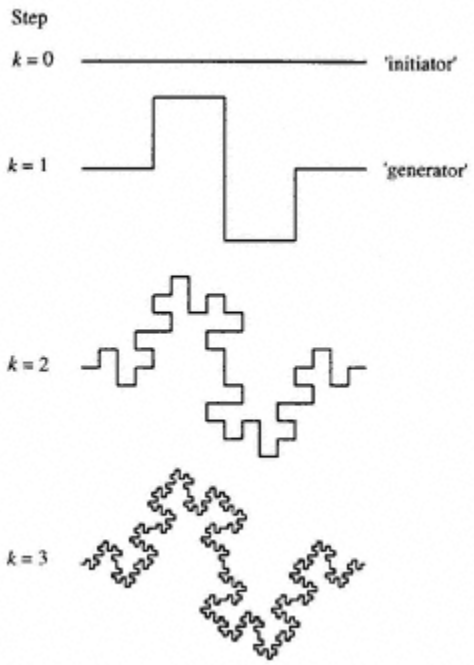

Figure 2.12.
The first three stages in the
construction of the quadratic Koch curve.

2.6—
The Quadratic Koch Curve

The Koch curve shown in both figures 2.10 and 2.11 is more specifically known as the triadic Koch curve. As with the triadic Cantor set, the triadic Koch curve's name stems from the fact that the middle thirds of the line segments are modified at each step. By changing the form of the generator a variety of Koch curves may be produced. Figure 2.12 contains the first three stages in the construction of the quadratic Koch curve, also known as the Minkowski sausage. This curve is generated by repeatedly replacing each line segment, composed of four quarters, with the generator consisting of eight pieces, each one quarter long (see figure 2.12). As with the triadic Koch curve the Minkowski sausage is a fractal object. Each smaller segment of the curve is an exact replica of the whole curve. There are eight such segments making up the curve, each one a one-quarter reduction of the original curve. Thus, $N = 8$, $\varepsilon = \frac{1}{4}$, and the similarity dimension based on expression (2.3) is

$$D_S = \frac{\log(N)}{\log(1/\varepsilon)} = \frac{\log(8)}{\log(4)} = \frac{3\log(2)}{2\log(2)} = \frac{3}{2} = 1.5. \qquad (2.6)$$

Figure 2.13 contains four more Koch curves produced using a variety of generators. The reader is invited to define his, or her, own generators, and use them to produce new fractal curves.

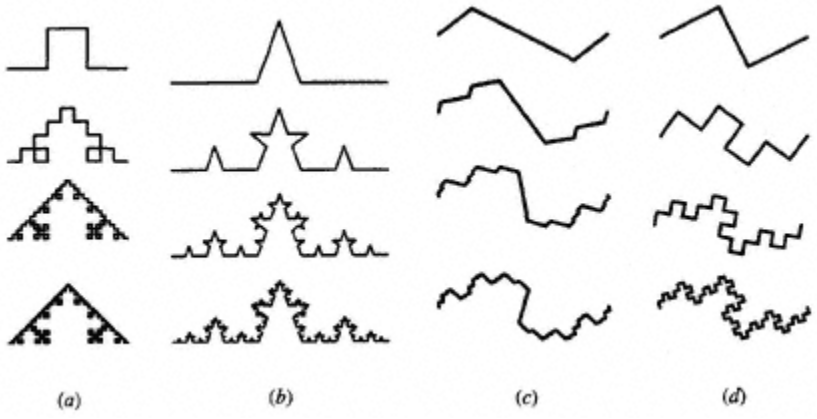

Figure 2.13.
Miscellaneous Koch curve constructions (all have unit line initiators—not shown).

2.7—
The Koch Island

The Koch island (or snowflake) is composed of three Koch curves rotated by suitable angles and fitted together: its construction is shown in figure 2.14. We already know that the length of the Koch curve is immeasurable, so the length of the coastline of the Koch island is seemingly infinite, but what about the area bounded by the perimeter of the island? It certainly looks finite. We can obtain a value for the bounded area by examining the construction process. Let us first assume for simplicity that the initiator is

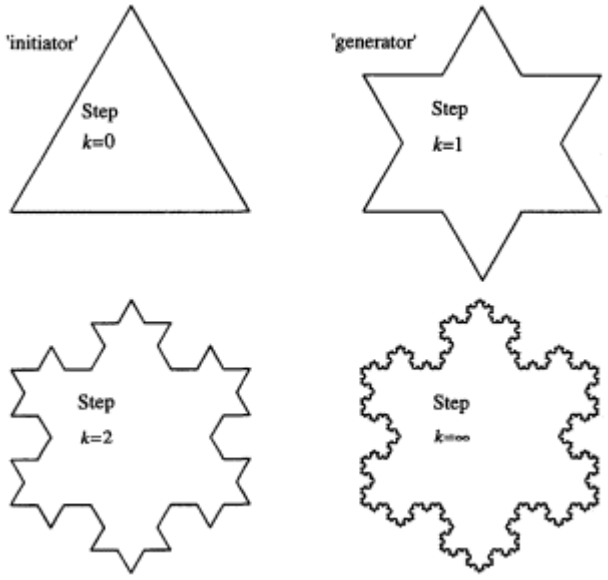

Figure 2.14.
The Koch island and its construction.

composed of three unit lines. The area bounded by the perimeter is then half of the base multiplied by the height of the equilateral triangle, i.e. $\frac{1}{2} \times 1 \times \sqrt{3}/2$. At step $k = 1$ three smaller triangles are added, each with a base length equal to one third. At step $k = 2$ another twelve smaller triangles are added, each with base length equal to one ninth. At step $k = 3$ (not shown in the figure) forty-eight smaller triangles are added, each with base length of one twenty-seventh. The area then increases at each stage as follows:

$$\text{step } k = 0 \quad \text{area} = \frac{1}{2} \times \frac{\sqrt{3}}{2} \times 1 = \frac{\sqrt{3}}{4} \tag{2.7a}$$

$$\text{step } k = 1 \quad \text{area} = \frac{\sqrt{3}}{4} + 3\left(\frac{\sqrt{3}}{4 \times 3} \times \frac{1}{3}\right) \tag{2.7b}$$

$$\text{step } k = 2 \quad \text{area} = \frac{\sqrt{3}}{4} + 3\left(\frac{\sqrt{3}}{4 \times 3} \times \frac{1}{3}\right) + 12\left(\frac{\sqrt{3}}{4 \times 9} \times \frac{1}{9}\right) \tag{2.7c}$$

$$\text{step } k = 3 \quad \text{area} = \frac{\sqrt{3}}{4} + 3\left(\frac{\sqrt{3}}{4 \times 3} \times \frac{1}{3}\right) + 12\left(\frac{\sqrt{3}}{4 \times 9} \times \frac{1}{9}\right) + 48\left(\frac{\sqrt{3}}{4 \times 27} \times \frac{1}{27}\right) \tag{2.7d}$$

In general, for an arbitrary step k

$$\text{Area} = \frac{3 \times \sqrt{3}}{4 \times 4}\left(\frac{4}{3} + \frac{4^1}{9^1} + \frac{4^2}{9^2} + \frac{4^3}{9^3} + \ldots + \frac{4^k}{9^k}\right). \tag{2.7e}$$

We may then split up this expression to give

$$\text{area} = \frac{3 \times \sqrt{3}}{16}\left(\frac{1}{3}\right) + \frac{3 \times \sqrt{3}}{16}\left(1 + \frac{4^1}{9^1} + \frac{4^2}{9^2} + \frac{4^3}{9^3} + \ldots + \frac{4^k}{9^k}\right). \qquad (2.7f)$$

In the limit, as k tends to infinity, the geometric series in the brackets on the right-hand side of the above expression tends to $\frac{9}{5}$: this leaves us with an area of

$$\text{area} = \frac{3 \times \sqrt{3}}{16}\left(\frac{1}{3} + \frac{9}{5}\right) = \frac{3 \times \sqrt{3}}{16} \times \frac{32}{15} = \frac{2}{5}\sqrt{3}. \qquad (2.7g)$$

The Koch island therefore has a finite area of $\frac{2}{5}\sqrt{3}$, or about 0.693 units (of area). Thus, the Koch island has a regular area, in the sense that it is bounded and measurable, but an irregular, immeasurable perimeter. To generate the Koch island, we used three Koch curves with unit initiator. However, if the initiator were a in length, then the area would be simply $\frac{2}{5}\sqrt{3}a^2$. You can easily verify this for yourself. We will return briefly to the Koch island in our discussion of the fractal nature of natural coastlines in the next chapter.

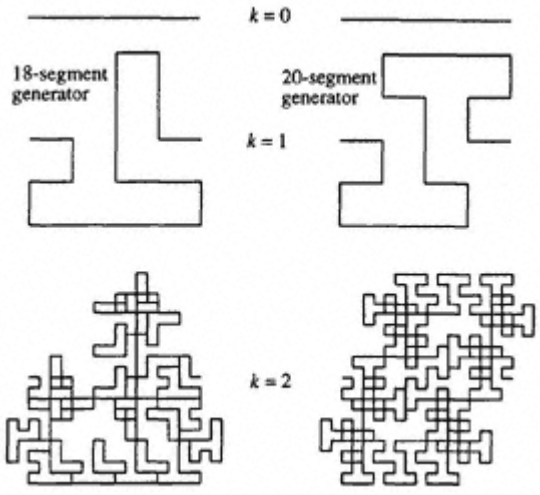

Figure 2.15.
The construction process for curves with similarity dimension greater than two.

2.8— Curves in the Plane with Similarity Dimension Exceeding Two

The similarity dimension can exceed two for curves in the plane. This may initially seem counter-intuitive, however, it may be easily demonstrated. Figure 2.15 contains two curves whose generators replace the original line segments with curves consisting of eighteen and twenty segments respectively, each of side length one quarter of the original. The similarity dimension of the curve resulting from the eighteen-segment generator is

$$D_S = \frac{\log(N)}{\log(1/\varepsilon)} = \frac{\log(18)}{\log(4)} = 2.0849\ldots. \qquad (2.8)$$

Similarly, $D_S = 2.1609\ldots$ for the twenty-segment curve. The similarity dimension exceeds two in these cases due to the overlapping parts of the fractal curve. Here, for both curves we have the slightly unusual condition that $D_S > D_E > D_T$, however, as the fractal dimension exceeds the topological dimension the object is still fractal by our definition. One way to avoid the fractal dimension exceeding D_E is to use alternative definitions of dimension which only count overlapping parts of the curve once. These will be explored in the next chapter.

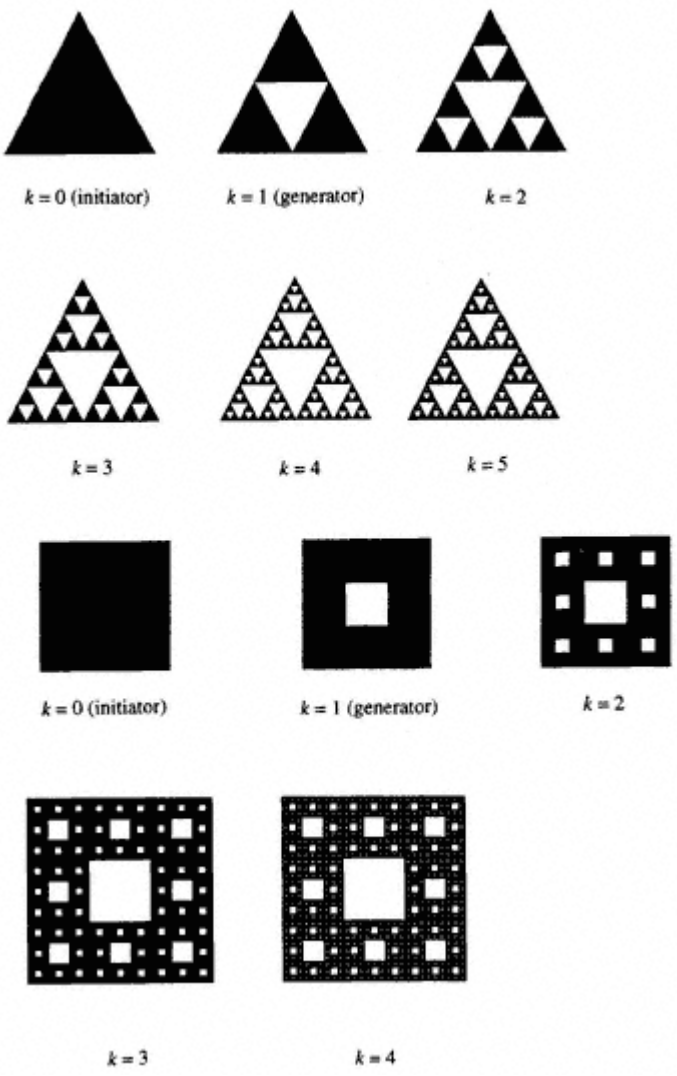

Figure 2.16.
Construction of the Sierpinski gasket (top) and carpet (bottom).

2.9—
The Sierpinski Gasket and Carpet

The construction of the **Sierpinski gasket** is illustrated in figure 2.16. The initiator in this case is a filled triangle in the plane. The middle triangular section is removed from the original triangle. Then the middle triangular sections are removed from the remaining triangular elements and so on. After infinite iterations the Sierpinski gasket is formed. Each prefractal stage in the construction is composed of three smaller copies of the preceding stage, each copy scaled by a factor of one half. The similarity dimension is given by

$$D_S = \frac{\log(N)}{\log(1/\varepsilon)} = \frac{\log(3)}{\log(2)} = 1.5849\ldots . \qquad (2.9)$$

A sister curve to the Sierpinski gasket is the **Sierpinski carpet** also shown in figure 2.16. Its method of construction is similar to that of the gasket: this time the initiator is a square and the generator removes the middle square, side length one-third, of the original square. With both the Sierpinski gasket and carpet, the constructions lead to fractal curves whose area vanishes.

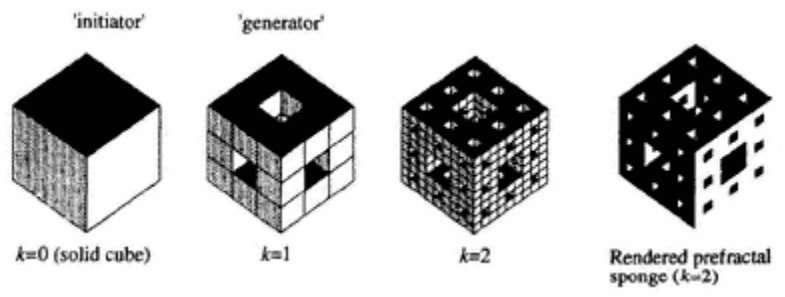

Figure 2.17.
Constructing the Menger sponge.

2.10—
The Menger Sponge.

So far we have looked at constructions on the line (Cantor set) and in the plane (Koch curve and Sierpinski gasket and carpet). We end this chapter with an interesting object constructed in 3D space—the **Menger sponge.** Its construction is shown in figure 2.17 and, as can be seen, it is closely related to the Sierpinski carpet. The initiator in the construction is a cube. The first iteration towards the final fractal object, the generator, is formed by 'drilling through' the middle segment of each face. This leaves a prefractal composed of twenty smaller cubes each scaled down by one-third. These cubes are then drilled out leaving 400 cubes scaled down by one-ninth from the original cube (step $k = 2$ in the figure). Repeated iteration of this construction process leads to the Menger sponge. The similarity dimension of the Menger sponge is

$$D_S = \frac{\log(N)}{\log(1/\varepsilon)} = \frac{\log(20)}{\log(3)} = 2.7268\ldots \qquad (2.10)$$

which is between its topological dimension of one (as it is a curve with zero volume, zero area and infinite length) and Euclidean dimension of three.

2.11— Chapter Summary and Further Reading

2.11.1— Chapter Keywords and Key Phrases

exact self-similarity	*regular fractals*	*fractal dimension*
Cantor set	*initiator*	*generator*
prefractals	*Euclidean dimension*	*topological dimension*
similarity dimension	*Koch curve*	*Sierpinski gasket/carpet*
Menger sponge		

2.11.2— Summary and Further Reading

In this chapter we have been introduced to regular fractal objects which have exact self-similarity at all scales, i.e. each small part of the object contains identical copies of the whole. To characterize these fractals requires that we re-evaluate our concepts of dimension. The Euclidean and topological definitions of dimension give only integer values. To obtain a fractal dimension for the exactly self-similar fractals we used, possibly the simplest definition of fractal dimension, the similarity dimension, D_S. In general, if the similarity dimension is greater than the topological dimension of the object then the object is a fractal, and, more often than not, the fractal dimension is a non-integer value. For more examples and information on exactly self-similar fractals the reader is referred for an elementary introduction to the book by Lauwerier (1991), and for an intermediate and comprehensive introduction to the book by Mandelbrot (1977), or, better, the extended version of this text by Mandelbrot (1982a). In-depth accounts of the Cantor set, Koch curve, Sierpinski gasket and Menger sponge, together with brief biographical details of their originators, are given by Peitgen *et al* (1992a). A method for the generation of the Sierpinski gasket using random numbers is given, amongst other useful information, by Peitgen *et al* (1991). Reiter (1994) presents some computer generated generalizations of the Sierpinski gaskets and carpets and the Menger sponge. The computer generation of the Koch curve is discussed by Hwang and Yang (1993). David (1995) presents two examples of 3D regular fractals based on Keplerian solids and Wicks (1991) presents an advanced mathematical account of fractals and hyperspaces.

Much of the interest in fractal geometry lies in its ability to describe many natural objects and processes, however, generally these are not exactly self-similar but rather statistically self-similar, whereby each small part of the fractal has the same statistical properties as the whole. We move on to these statistical, or random, fractals in the following chapter.

2.12— Revision Questions and Further Tasks

Q2.1 List the keywords and key phrases of this chapter and briefly jot down your